Combustion Wave Structures of Ammonium Perchlorate Composite Propellants

N. Kubota*
Japan Defense Agency, Tachikawa, Tokyo, Japan
T. Kuwahara† and S. Miyazaki†
Nissan Motor Co., Ltd., Suginami, Tokyo, Japan
K. Uchiyama‡
Nippon Oil and Fats Co., Ltd., Taketoyo, Aichi, Japan
N. Hirata§
Daicel Chemical Industries, Ltd., Ibogawa, Hyogo, Japan

The combustion wave structures of ammonium perchlorate composite propellants have been studied experimentally by means of thermal analysis and microthermocouple techniques. Two types of binders are used in order to examine the impact of binders on the burning rate characteristics. The binders used are hydroxy terminated polybutadiene (HTPB) and hydroxy terminated polyester (HTPE). The oxygen concentration of the HTPE is much higher than that of the HTPB. The results of thermal analysis show that HTPB decomposes exothermically and HTPE decomposes endothermically. The reaction time in the gas phase just above the burning surface is calculated based on the data obtained by the temperature distribution measurements in the combustion waves. The reaction rate of HTPE propellant is found to be higher than that of the HTPB propellant. Though the heat feedback from the gas phase to the burning surface of the HTPB propellant is smaller than that of HTPE propellant, the burning rate of HTPB propellant appears to be higher than that of HTPE propellant. The results obtained show that the chemical properties of binders play an important rôle not only in the reaction rate in the gas phase but also in the heat release at the burning surface.

Introduction

NUMEROUS experimental and theoretical studies have been done on the combustion of ammonium perchlorate (AP) composite propellants. The primary objective of these studies is to deduce enough information about the combustion mechanism to predict the burning rate characteristics. Since AP composite propellants consist of finely divided AP particles bonded in a matrix of polymetric fuel binder, the combustion wave structure on and above the burning surface of the propellants becomes very heterogeneous. The decomposition gases generated from AP particles and the binder yield diffusional flamelets in the gas phase. Thus, the heat feedback from the gas phase to the burning surface is largely dependent not only on the chemical reaction in the gas phase but also on the diffusional process of the decomposed gases.

Since the burning rate of the propellants is determined by the heat feedback from the gas phase to the burning surface and the heat generated in the condensed phase, the burning rate can be controlled by changing the AP particle size. Furthermore, the burning rate can be altered by the addition of catalysts that act on the reaction zones in the gas phase and/or the condensed phase. For example, iron oxide is used to increase the burning rate, and lithium fluoride to decrease it. However, the range of the burning rate change by means of changes in the particle size of AP or of added burning rate catalysts is limited.

The binder in composite propellants has been considered with a view to increasing its mechanical properties and to making its oxidizer/fuel ratio as close as possible to the stoichiometric ratio. There have been very limited studies of the impact of binders on the burning rate of composite propellants.[1-7] It has been reported that binders have an important effect on the burning rate.[8] For example, the addition of carborane within a binder as a plasticizer increases the burning rate of AP composite propellants by about four times.

Thus, in this study the effect of binders on the burning rate of AP composite propellants was determined in order to gain a wide spectrum of burning rate. Furthermore, the flame structure was examined using two different types of binder. The measurements of temperature profiles in the combustion wave were done in order to elucidate the physical and chemical processes of propellant combustion.

Binder and Propellant Formulation

In order to evaluate the effect of binders on the burning rate of AP composite propellants and on the flame structure of the propellants, the following two types of prepolymers were used: hydroxy terminated polybutadiene (HTPB) and hydroxy terminated polyester (HTPE). Both prepolymers were cured with isophorondiisocianate (IPDI). The chemical structures of the prepolymers are shown in Fig. 1, and the detailed physical and chemical properties of the binders are shown in Table 1. It is shown that HTPB contains low oxygen concentration and HTPE contains high oxygen concentration. Furthermore, the chemical structures of these two binders are characterized with chemical bonds as shown in Fig. 1. The HTPB binder is characterized by carbon-carbon double bonds, and the HTPE binder is characterized by ester bonds and carbon-carbon single bonds.

Two types of propellants were formulated using HTPB and HTPE binders. Two types of propellants were made with 16% binder and 84% AP. The AP particles used were a bimodal

---

Received June 6, 1984; revision submitted March 6, 1986.

*Chief, Rocket Propulsion Laboratory, Third Research Center, Technical Research and Development Institute. Member AIAA.

†Research Engineer, Aeronautical & Space Division.

‡Chemist, Solid Propellant Research Division, Taketoyo Plant.

§Chemist, Solid Propellant Research Division, Harima Plant.

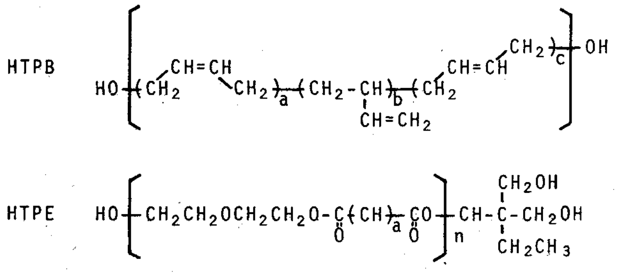

Fig. 1 Chemical structures of HTPB and HTPE prepolymers used in this study.

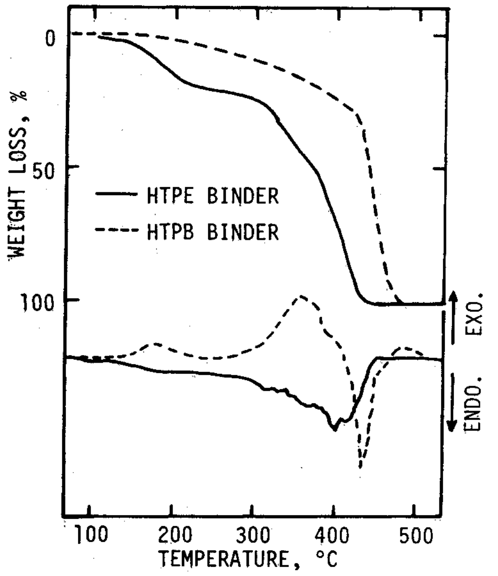

Fig. 2 TGA and DTA results of HTPB and HTPE binders, showing that the HTPB binder decomposes exothermically and the HTPE binder decomposes endothermically.

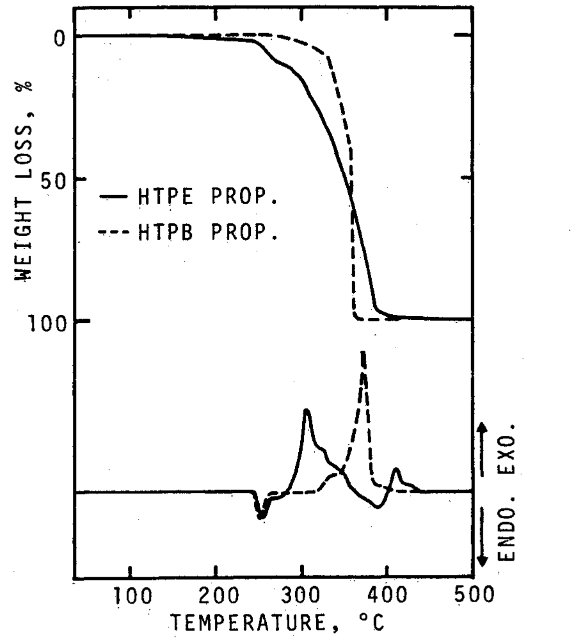

Fig. 3 TGA and DTA results of HTPB and HTPE propellants.

Table 1 Chemical properties of HTPB and HTPE binders

Binder	ΔH_f[a]	$\Psi(O)$[b]	Chemical formula
HTPB	−13.8	3.6	$C_{7.075}H_{10.647}O_{0.223}N_{0.063}$
HTPE	−131	34.1	$C_{4.763}H_{7.505}O_{2.131}N_{0.088}$

[a]Heat of formation (25°C), Kcal/mole. [b]Oxygen concentration, % by weight.

mixture of a large-sized AP and a small-sized AP. The composition of these two types of propellants is shown in Table 2. In addition to these propellants, several types of propellants were also made in order to understand the effect of AP particle size on the gas phase structure.

Experimental

In order to evaluate the thermal properties of these binders and propellants, thermogravimetric analysis (TGA) and differential thermal analysis (DTA) were employed. Both experiments were conducted at 1 atm pressure in helium. The heating rates of the TGA and DTA were varied from 1 to 25°C/min in order to gain kinetic parameters of the decomposition of the binders and propellants. The weight of the samples used was about 10 mg for each test.

Burning rates of the propellants were measured with a chimney-type strand burner, which was pressurized with nitrogen. The size of the strand samples was 7×7×70 mm, and three low melting-point fuse wires (0.25 mm in diameter) were threaded through each strand for the measurement of the burning time. The burning rates at subatmospheric pressure were also measured with the same strand burner. A vacuum pump was used to lower the pressure in the burner, and nitrogen gas was supplied from the side of the burner to adjust the pressure in the burner.

The combustion wave structures were measured with microphotography and microthermocouples. The flame structures of the propellants at subatmospheric pressures were photographed through a transparent window, which was mounted on the side of the burner. The temperature distributions in the combustion waves were measured with microthermocouples (Pt-Pt10%Rh 2.5 μm in diameter and 25 μm diameter wires) which were embedded in the strand samples. The measurement techniques are described elsewhere.[9]

Thermal Decompositions of Binders and Propellants

Typical TGA and DTA curves of HTPB and HTPE binders in helium atmosphere are shown in Fig. 2. The HTPB binder decomposes exothermically at 140-410°C, and an endothermic reaction occurs at about 440°C. On the other hand, the HTPE binder decomposes endothermically at 90-450°C. No exothermic reaction is observed for the decomposition of the HTPE binder.

As shown in Fig. 2 both HTPB and HTPE binders decompose in two-stage reactions. The first-stage reaction of the HTPB binder occurs at 140-420°C, and 30% of weight decomposes to gases. The second-stage reaction occurs at 420-480°C, and the remaining 70% of weight decomposes to gases. The maximum weight loss of the HTPB binder appears at about 435°C, and the decomposition is completed at about 500°C.

The first-stage reaction of the HTPE binder occurs at 90-270°C, and 20% of weight decomposes to gases. The second-stage reaction occurs at 270-420°C, and the remaining 80% of weight decomposes to gases. The maximum weight loss of the HTPE binder appears at about 405°C, and the decomposition is completed at about 450°C.

The TGA and DTA curves of HTPB and HTPE propellants are shown in Fig. 3. The TGA curves show that the HTPE propellant decomposes more slowly than the HTPB propellant. The 50% of weight loss temperature is 350°C for the HTPE propellant and 360°C for the HTPB propellant. The endothermic peak is observed at 245°C for both propellants. This endothermic peak is caused by the crystal transformation of AP from orthorhombic to cubic structures.[10]

The maximum exothermic peak is 300°C for the HTPE propellant and 370°C for the HTPB propellant. An endothermic

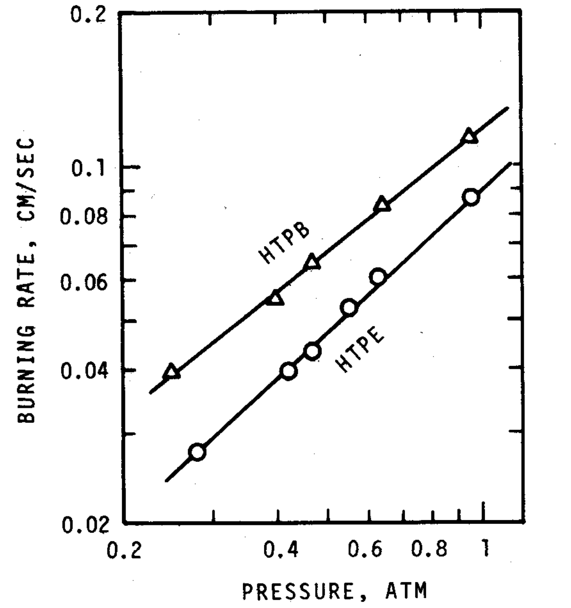

Fig. 4 Burning rate characteristics of HTPB and HTPE propellants at low-pressure region.

Table 2 Propellant compositions tested in this study

Propellant	Binder	AP (200μ)	AP (20μ)	T_f^a
HTPE	16 (HTPE)	42	42	2546
HTPB	16 (HTPB)	42	42	2557

[a]Adiabatic flame temperature at 0.5 atm, K.

reaction occurs at 360-400°C for the HTPE propellant. However, no endothermic reaction occurs for the HTPB propellant.

Burning Rate

As shown in Figs. 4 and 5, the burning rates of HTPB and HTPE propellants are characterized by low- and high-pressure regions. At a low-pressure region below 1 atm, the burning rates of both propellants increase linearly with increasing pressure in log (pressure) vs log (burning rate) plots. The pressure exponents of HTPB and HTPE propellants are 0.79 and 0.96, respectively. It is evident that the burning rate characteristics are dependent on the type of binder used.

At high-pressure regions above 10 atm, the effect of binders on the burning rate characteristics is clear. The burning rate of the HTPB propellant increases with increasing pressure, and the pressure exponent is 0.51 above 10 atm. However, the burning rate of the HTPE propellant becomes less pressure dependent and the pressure exponent decreases with increasing pressure. When pressure is further increased, burning interruption occurs at about 120 atm.

Temperature Distribution in the Combustion Wave

The combustion processes of the propellants were studied through temperature measurements in the combustion waves. The temperature rise of both HTPB and HTPE propellants was rapid above the burning surface, making the temperature gradient in the reaciton zone too steep to measure accurately. The measurements, however, provided considerable information about the effects of binders in the combustion wave. In general, the reaction rate of a gaseous mixture becomes slow at low pressures, and the thickness of the reaction zone increases with decreasing pressure. Thus, the temperature measurements were conducted at low pressures below 1 atm in order to obtain information as detailed as possible.

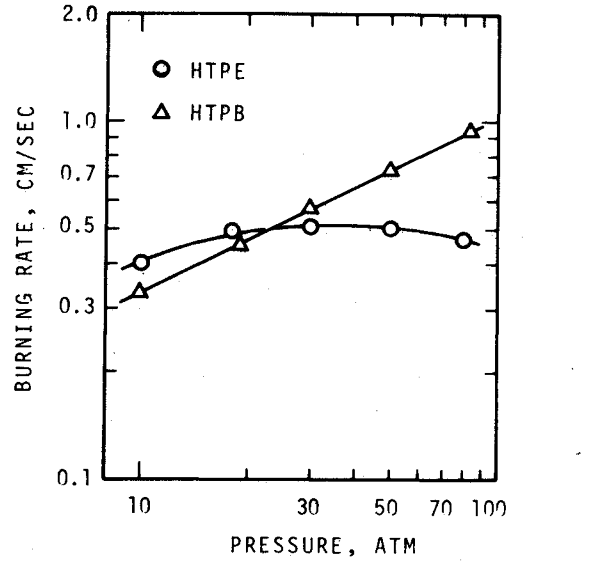

Fig. 5 Burning rate characteristics of HTPB and HTPE propellants at high-pressure region.

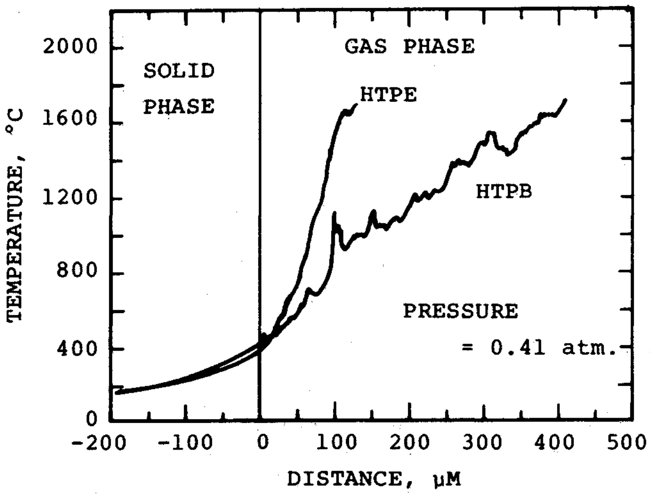

Fig. 6 Typical temperature profiles in the combustion waves (zones I and II) of HTPB and HTPE propellants at low-pressure region.

Figure 6 represents a typical trace produced by an oscillograph of the distribution of temperature in the combustion wave. In all the temperature traces, it is possible to distinguish the following three zones. Zone I is a nonreacting zone where only pure heat conduction occurs. Zone II is an exothermic reaction zone, which extends from the burning surface to the region at which temperature gradient becomes small. Zone III is a flame zone where the temperature reaches maximum and remains approximately constant.

A relatively large spike in the temperature signaling appears at the end of zone I, which is defined as the burning surface of the propellant. The several observed temperature spikes in zone II are believed to be caused by a number of flame streams generated by the diffusion flames produced by each AP particle and the binder surrounding the AP particle. The temperature spikes diminished downstream in the gas phase. This is because the diffusion flame streams emerged and formed a homogeneously mixed flame zone (zone III). The results described above were confirmed with the experiments using various types of AP propellants made from different AP concentrations. The number of temperature spikes decreased

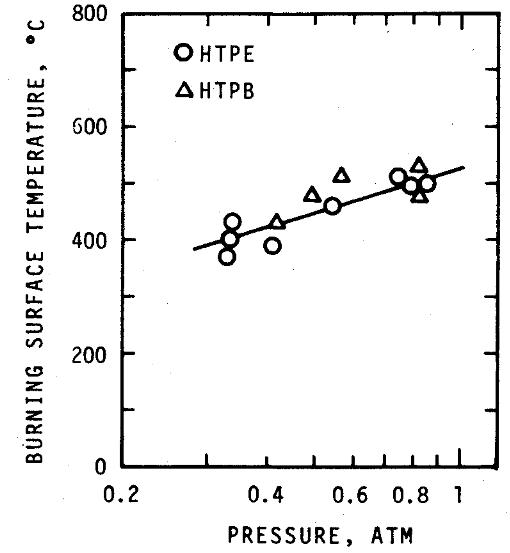

Fig. 7 Burning surface temperatures of HTPB and HTPE propellants, showing no clear difference of T_s between HTPB and HTPE propellants.

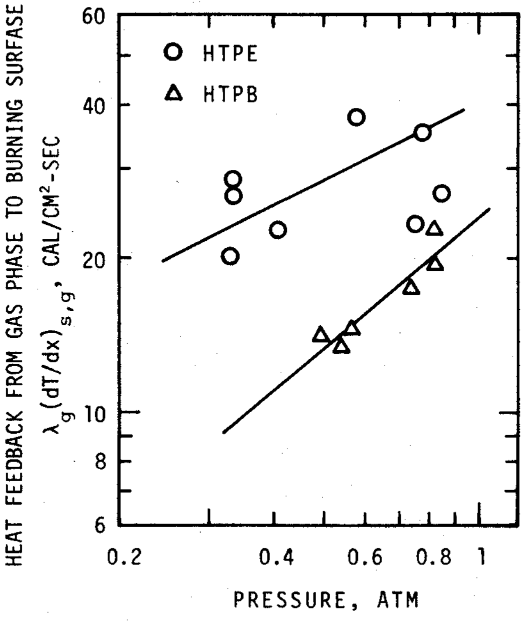

Fig. 8 Heat feedback from the gas phase to the burning surface of HTPB and HTPE propellants, showing higher heat flux of HTPE propellant than that of HTPB propellant.

when large-sized AP (400 μm-diam) particles were used and also decreased when the concentration of AP was decreased.

In order to evaluate the effects of gas phase and condensed phase reactions on the burning rate, the following heat balance equation at the burning surface can be applied to the measurement results:

$$\rho_p r c_p (T_s - T_0) + \rho_p r Q_s = \lambda_g \left(\frac{dT}{dx}\right)_{s,g}$$

where λ is thermal conductivity, ρ density, c heat capacity, r burning rate, T temperature, x distance, Q_s the heat release at the burning surface (exothermic or endothermic), subscript p propellant, s burning surface, g gas phase, 0 initial condition, and s,g the gas phase at the burning surface.

Figure 7 shows the results of the burning surface temperature vs pressure relationship obtained from the temperature distribution measurements. The burning surface temperature was determined by the so-called "temperature inflection method" described in Ref. 9. The surface temperature increases with increasing pressure for both HTPB and HTPE propellants. No clear difference in the burning surface temperature was seen between these two types of propellants.

Since the determination of the heat flux from the gas phase to the burning surface is in the center of the research of propellant combustion mechanism, the measurements of the temperature gradient in zone II were conducted using the temperature profile traces. The temperature gradient was defined as an averaged value of the gradient which excludes the temperature spikes.

The $q_{s,g} = \lambda_g (dT/dx)_{s,g}$ was determined from the results of the temperature profile measurements. The results are shown in Fig. 8. The scatter in the data is high because of the heterogeneous structure in zone II. The $q_{s,g}$ for both propellants increases with increasing pressure. Figure 9 shows the calculated results of Q_s based on the heat balance equation at the burning surface and the data shown in Figs. 7 and 8. The physical parameters used for the calculation were $\lambda_g = 2.0 \times 10^{-4}$ cal/cm-s-K, $\rho_p = 1.66$ g/cm³, and $c_p = 0.30$ cal/g-K for both propellants. The Q_s of the HTPB propellant is relatively pressure-independent and appears to be exothermic below 1 atm. However, the Q_s of the HTPE propellant increases with increasing pressure and appears to be endothermic below 1 atm.

Discussion of Combustion Wave Structures

Though the heat feedback from the gas phase to the burning surface of HTPB propellant is smaller than that of the HTPE propellant, the burning rate of the HTPB propellant is greater than that of the HTPE propellant. These results are seen from Figs. 8 and 4. In order to understand the reaction mechanisms in the combustion waves, the reaction time in the gas phase just above the burning surface is evaluated.

The reaction time can be represented by

$$\tau_g = L_g / u_g$$

where τ_g is the reaction time, L_g the thickness of the reaction zone, and u_g the gas flow velocity in the reaction zone. The thickness of the reaction zone is given by

$$L_g = \frac{T_s - T_s}{(dT/dx)_{s,g}}$$

Using the mass continuity relation at the burning surface and the equation of state in the gas phase, the reaction time is given by

$$\tau_g = \frac{T_g - T_s}{r \rho_p} \frac{p}{R T_g (dT/dx)_{s,g}}$$

where R is the gas constant in the reaction zone.

The calculated results of τ_g for both HTPB and HTPE propellants are shown in Fig. 10. In the computations of τ_g, the $(dT/dx)_{s,g}$ and T_s obtained from the temperature profile measurements were used. The gas constant R was assumed to be 3.2×10^3 g-cm/g-K. The τ_g was defined as the reaction time needed to raise the gaseous species temperature from the burning surface temperature T_s to the temperature $T_g = 1500$ K.

As shown in Fig. 10, the reaction time in the gas phase decreases with increasing pressure. The τ_g of the HTPE propellant is smaller than that of the HTPB propellant. These results indicate that the gas phase reaction rate of the HTPE propellant is greater than that of the HTPB propellant.

In general, the reaction rate of a gaseous mixture depends largely on its fuel/oxidizer mixture ratio. The reaction rate increases as the mixture ratio approaches the stoichiometric ratio. Since the oxygen concentration of the HTPE binder is high, as shown in Table 1, the decomposed gases generated from the HTPE binder at the burning surface contain suffi-

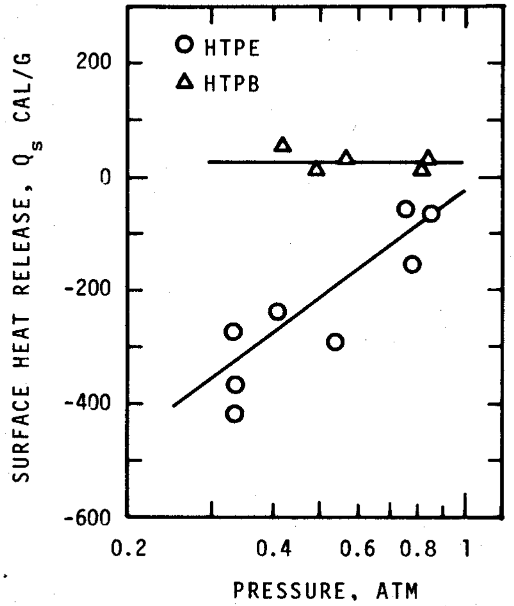

Fig. 9 Surface heat release of HTPB and HTPE propellants showing higher surface heat release of HTPB propellant than that of HTPE propellant at low-pressure region.

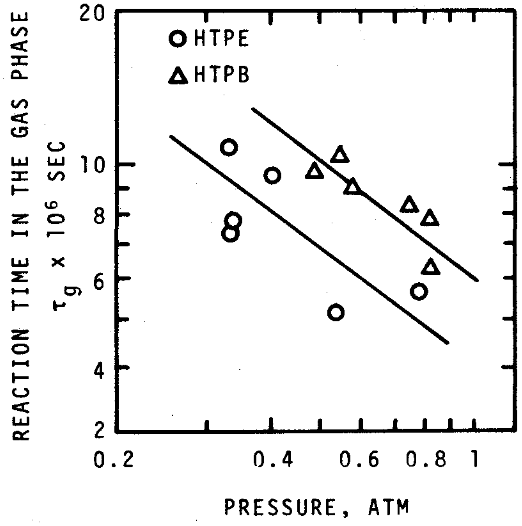

Fig. 10 Reaction time in the gas phase just above the burning surface for HTPB and HTPE propellants.

cient oxygen fragments to react with the remaining fuel fragments. Thus, the decomposed gases can react exothermically at the burning surface due to the diffusional mixing of the gases generated from the surrounding AP particles. Consequently, the reaction rate of the HTPE propellant in the gas phase just above the burning surface is probably increased by the increased reaction rate of the HTPE binder when compared with the case of the HTPB binder.

On the other hand, as shown in Fig. 9, the heat release at the burning surface Q_s of the HTPB propellant is greater than that of the HTPE propellant. Since the concentration of the AP contained in the propellant is the same for both HTPB and HTPE propellants, the difference of Q_s between HTPB and HTPE propellants is caused by the difference of the chemical properties between HTPB and HTPE binders. It is evident from the measurement results of thermal analysis shown in Fig. 2 that the HTPB binder decomposes exothermically and the HTPE binder decomposes endothermically. Thus, one can conclude that the greater Q_s of the HTPB propellant is caused by the exothermic reaction of HTPB binder when compared with the HTPE propellant, whose binder decomposes endothermically. Since the burning rate of propellants is determined by the heat generated at the burning surface and the heat feedback from the gas phase to the burning surface, the observed burning rate characteristics of HTPB and HTPE propellants shown in Fig. 4 can be understood from the results obtained in this study.

Summary

The temperature gradient in the gas phase just above the burning surface was measured at subatmospheric pressure in order to obtain information on combustion waves as detailed as possible. The results obtained show that the reaction rate in the gas phase of the HTPE propellant is greater than that of the HTPB propellant. Therefore, the heat feedback from the gas phase to the burning surface of the HTPE propellant is greater than that of the HTPB propellant. However, the burning rate of the HTPE propellant appears to be lower than that of the HTPB propellant.

On the other hand, the results of the measurements of the condensed phase reaction indicate that the heat release at the burning surface is greater for the HTPB propellant when compared with the HTPE propellant. This difference is caused by the exothermic decomposition of the HTPB binder. Thus, the higher burning rate of the HTPB propellant, as compared to the HTPE propellant, is due to the greater heat release at the burning surface.

References

[1] Steinz, J. A., Stang, P. L., and Summerfield, M., "The Burning Mechanism of Ammonium Perchlorate-Based Composite Solid Propellants," AIAA Paper 68-658, 1968.

[2] Bastress, E. K., "Modification of the Burning Rates of Ammonium Perchlorate Solid Propellants by Particle Size Control," Ph.D. Thesis, Department of Aeronautical Engineering, Princeton University, Princeton, NJ, Jan., 1961.

[3] Beckstead, M. W., Derr, R. L., and Price, C. F., "A Model of Composite Solid-Propellant Combustion Based on Multiple Flames," *AIAA Journal*, Vol. 8, Dec. 1970, pp. 2200-2207.

[4] Hermance, C. E., "A Model of Composite Propellant Combustion Including Surface Heterogeneity and Heat Generation," *AIAA Journal*, Vol. 4, Sept. 1966, pp. 1629-1637.

[5] Kubota, N., "Physicochemical Process of HMX Propellant Combustion," Nineteenth Symposium (International) on Combustion, The Combustion Institute, Pittsburgh, PA, 1982, pp. 777-785.

[6] Kuwahara, T. and Kubota, N., "Combustion of RDX/AP Composite Propellants at Low Pressures," *Journal of Spacecraft and Rockets*, Vol. 21, Sept-Oct. 1984, pp. 502-507; also Kubota, N., Takizuka, M., and Fukuda, T., "Combustion of Nitramine Composite Propellants," AIAA Paper 81-1582, 1981.

[7] Kuwahara, T. and Kubota, N., "Low Pressure Burning of Ammonium Perchlorate Composite Propellants," *Combustion Science and Technology*, to be published.

[8] Hill, W. E. and Johnson, F. A., "Carborane Burning Rate Modifiers," Naval Sea Systems Command, Washington DC, Rept. N0024-76-PR-03309, AD-A035404, 1976.

[9] Sabadell, A. J., Wenograd, J., and Summerfield, M., "Measurement of Temperature Profiles Through Solid Propellant Flames Using Fine Thermocouples," *AIAA Journal*, Vol. 3, Sept. 1965, pp. 1580-1584.

[10] Caveny, L. H. and Pittman, C. U. Jr., "Contribution of Solid Phase Heat Release to Ammonium Perchlorate Composite Propellant Burning Rate," *AIAA Journal*, Vol. 6, Aug. 1968, pp. 1461-1467.